Simultaneous measurement of humidity and temperature based on a partially coated optical fiber long period grating

Aitor Urrutia[1], *Javier Goicoechea*[1], *Amelia L. Ricchiuti*[2], *David Barrera*[2], *Salvador Sales*[2], *and Francisco J. Arregui*[1].

1 Nanostructured Optical Devices Laboratory, Electrical and Electronic Engineering Department, Institute of Smart Cities, Public University of Navarra, Campus Arrosadia, 31006 Pamplona, Spain

2 Optical and Quantum Communications Group, iTEAM Research Institute, Universidad Politécnica de Valencia, Camino de Vera s/n, 46022 Valencia, Spain.

*email aitor.urrutia@unavarra.es

ABSTRACT

A humidity and temperature optical fiber sensor based on a long-period grating (LPG), which can provide simultaneous response to both magnitudes, is proposed and demonstrated via experiments. Previously, the LPG was fully coated with humidity sensitive nanostructured polymeric thin films by the Layer-by-Layer (LbL) nano assembly technique. Hence the surrounding refractive index was changed, so provoking wavelength shifts of the attenuation bands of the transmission spectrum. This fully coated LPG was exposed to relative humidity (RH) and temperature tests, varying from 20% to 80% RH and from 25 ºC to 85 ºC, respectively. Then, half of the LPG coating was chemically removed and this results in the splitting of the main attenuation band into two different contributions. When this semi-coated LPG was also exposed to RH and temperature tests, the new two attenuation bands

presented different behaviours for humidity and temperature. This novel dual-wavelength based sensing method enables the simultaneous measurement of RH and temperature using only one LPG.

KEYWORDS

Optical fiber sensors, humidity, temperature, long period grating, LbL assembly

1. INTRODUCTION

Relative humidity (RH) and temperature are two of the most important magnitudes which must be monitored and controlled in industry, food quality, human comfort or health applications among other fields. A great variety of devices have been developed for this purpose using diverse methods [1]. Sometimes these sensors have to work in harsh environments and are affected by corrosive agents or the presence of electromagnetic interferences (EMI). To overcome these problems, optical fiber sensors are attractive due to their specific advantages such as long lifetime, corrosion free, light weight, EMI immunity, or remote sensing [2], [3], [4].

Recently, optical fiber gratings are having an important growth due to their unique sensing properties [5]. More specifically, in long-period gratings (LPGs), where the grating period written on a single-mode fiber is generally in the range of 100 μm to 1 mm, there is a coupling of light between the guided core mode and various co-propagating cladding modes. This coupling produces a series of attenuation bands in the optical fiber transmission spectrum, each one centered at a different resonant wavelength (see Figure 1). These resonant wavelengths depend mainly on the effective index of the coupled modes and the grating pitch [6], [7]. Although LPGs were initially developed as rejection-band filters [8], they also present interesting characteristics for sensing. The central wavelength of each LPG resonance depends critically on the refractive index difference between the core and the cladding, and hence any variation caused by strain, temperature, or even changes in the external refractive index may cause large wavelength shifts in the resonances [5, 6, 9].

In the last decades, new deposition techniques such as Layer-by-Layer (LbL) nano assembly [10], sol-gel [11], sputtering [12], or electrospinning [13] have enabled the fabrication of thin films and nanostructured sensitive coatings onto optical fiber structures. Diverse optical fiber sensors based on LPGs have been recently developed to monitor different physical and chemical magnitudes as humidity [14, 15], temperature [16], pH [17], hydrogen [18, 19], ethanol [20], ammonia [21], volatile organic compounds [22] and proteins [23], among others [24].

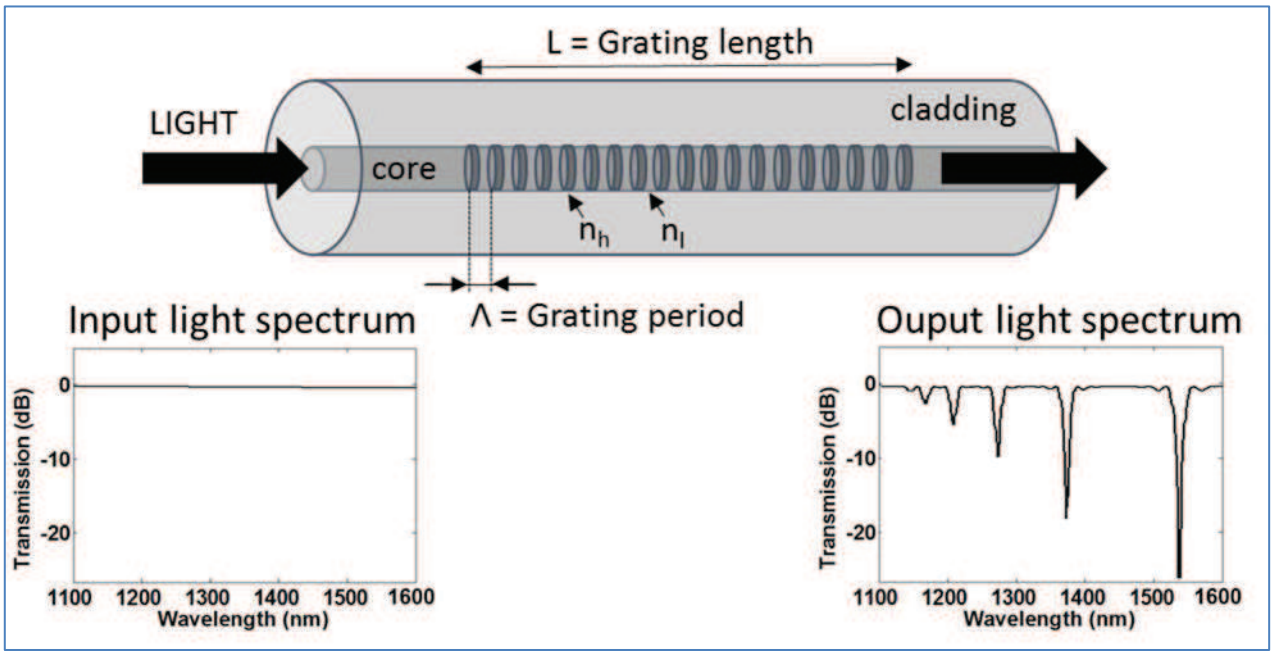

Figure 1. Scheme of a LPG, indicating their parameters, and its characteristic spectrum when the light goes through the grating.

Different approaches have successfully designed sensors for two or more magnitudes thanks to the use of more than one grating along the optical fiber, as the work presented by Viegas et al [25], where RH and temperature were simultaneously measured by the combination of a LPG and a fiber Bragg grating. In some reports, Mach-Zehnder interferometers based on two LPGs are able to sense temperature, external refractive index, and ammonia concentrations [26] at the same time. In other approach, one grating was combined with a Fabry-Perot interferometer [27] to sense also RH and temperature simultaneously.

Other authors have studied how some modifications in LPGs overlays can generate and tune the loss fringes in the output light spectrum [28]. Moreover, a theoretical study [29] has recently proposed the possibility of partially coated LPGs for sensing applications.

In this work, a novel approach for humidity and temperature sensing based on a half-coated LPG, is presented. To our knowledge, this is the first time that a LPG is partially coated to develop a sensing device. In addition, this new sensor provides a simultaneous response for two different external magnitudes using only one fiber grating thanks to the partial coating.

2. MATERIAL AND METHODS

2.1. Chemical reagents and materials

Sodium hydroxide (NaOH), potassium hydroxide (1N volumetric solution, KOH), sulphuric acid (98%, H_2SO_4), hydrogen peroxide (H_2O_2), poly(allylamine hydrochloride) (Mw ~ 56,000, PAH), and poly(acrylic acid, sodium salt) 35 wt% solution in water (Mw ~15,000, PAA) were purchased from Sigma Aldrich. All reagents were of analytical grade and used without further purification. Ultrapure water (18.3 M cm) was obtained by reverse osmosis followed by ion exchange and filtration (Barnstead Nanopure Diamond). All solutions were prepared using ultrapure water. Both PAH and PAA solutions were prepared with a concentration of 10 mM, and adjusted to a pH 4.5.

PAH and PAA weak polyelectrolytes were chosen for the fabrication of the LbL coating because of their well-known hydrophilic nature. In particular, PAH/PAA thin films thickness is humidity-dependent due to their swelling/de-swelling behavior [30]. This swelling property produces morphological and effective refractive index variations in the resultant coating, thus provoking changes in the optical response of the LPG optical fiber sensor.

2.2. LPG fabrication

The LPG was performed using the point-by-point technique by means of an Argon-ion frequency-doubled laser at a wavelength of 244 nm and a high-precise translation stage with an accuracy of few

nanometers. The laser beam, with 50 µm in diameter, was focused onto the optical fiber to modify the refractive index of the core. The exposure time in each point was constant along the total length of the grating.

The employed optical fiber was PS1250/1500 (from Fibercore Inc.), and the resultant grating parameters were 464 µm for period and 6 cm for length, respectively.

Next, LPG was connected to a broadband light source in one extreme, and to an optical spectrum analyzer (OSA) in the other to measure the transmission spectrum and observe the main attenuation band created by the grating.

2.3. Experimental setup

The experimental setup shown in Figure 2 was used to monitor the coating deposition onto the LPG, the further partial removal of the coating, and the respective RH and temperature tests. The coating deposition process will be described in the next subsection, and the partial removal of the coating is presented in the Results and Discussion Section.

The grating sensor was submitted to several RH cycles using a programmable climatic chamber. The humidity tests consisted of a constant slope from 80% RH to 20% RH, and next, RH variation was inverted from 20% to 80%. This cyclic up-and-down profile was repeated 3 times. Temperature was kept at 25ºC during the whole RH cycles.

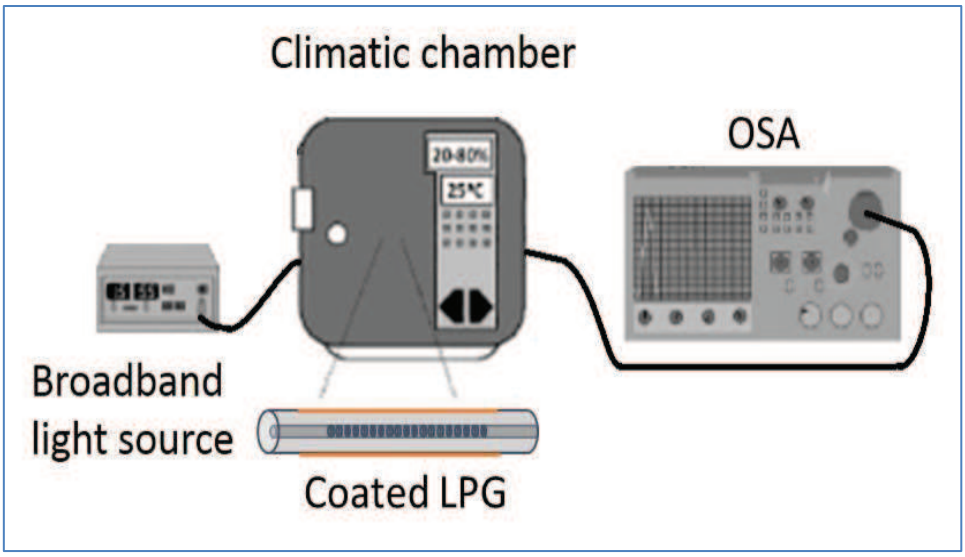

Figure 2. Experimental setup to monitor the optical sensor response.

Afterwards, the same setup was used to monitor the temperature. In this case, tests were performed like this: the RH was kept at a constant level of 30%RH while the temperature varied from 25ºC to 85ºC, and backwards.

All mentioned RH and temperature tests were previously performed with the original LPG, before coating it, thus taking these results as a reference. The same tests were also performed once the LPG is fully coated and, finally, after the partial removal of the coating.

2.4. Coating fabrication

LPG was coated with polymeric thin films by the LbL assembly method [10] using a ND-3D robot (from Nadetech Innovations Inc.) as follows. Briefly, LPG was cleaned with 0.1 M NaOH solution for 30 min and then treated with a 10 mM KOH solution for 5 min to charge the region surface negatively. Next, it was immersed in a positively charged PAH solution for 2 min and cleaned by several rinsing steps with ultrapure water. After that, the fiber was introduced in a negatively PAA solution for other 2 min, and then cleaned.

This deposition process was repeated 40 times, obtaining a final coating of 40 (PAH/PAA) bilayers onto the LPG surface. The building performance was monitored, recording the transmission spectrum after each bilayer was built. The evolution of the spectrum is plotted in Figure 3. The nanostructured coating caused a variation in the external refractive index, modifying the spectrum and the attenuation bands of the LPG. The original main attenuation band (centered in 1547 nm) was blue-shifted as the thin film was deposited, from 1547 nm to 1510 nm.

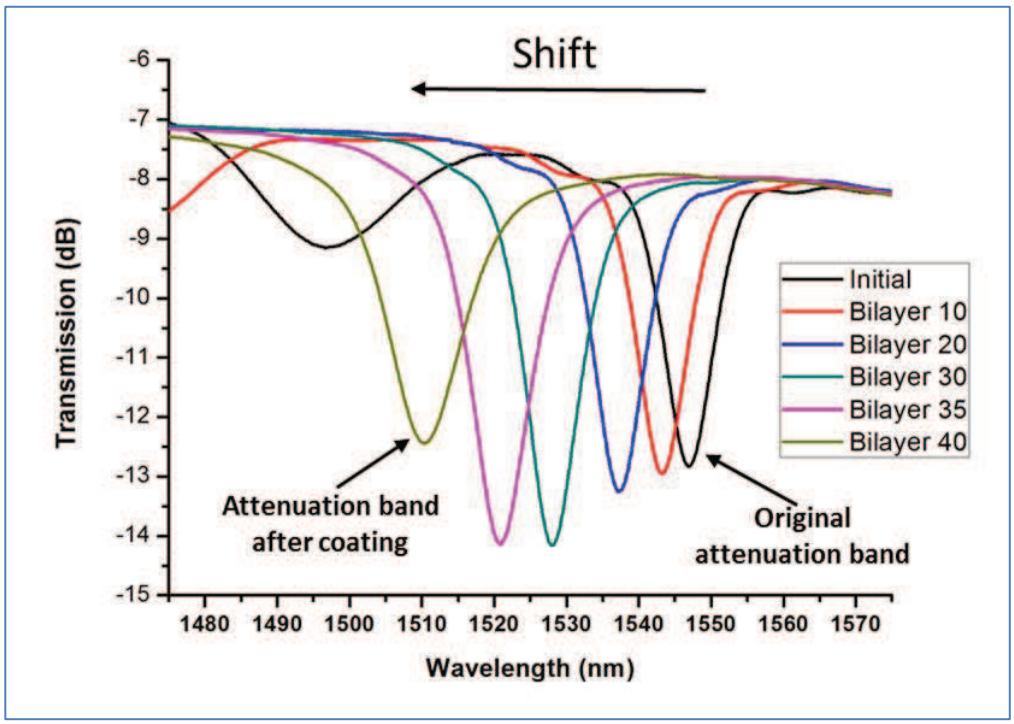

Figure 3. Evolution of the LPG spectrum for the main attenuation band during the LbL assembly process.

Once the deposition process was over, the coated LPG relaxed for 24 hours at room conditions. After this time, for the coating stabilization and drying, the main attenuation band remained centered in 1515 nm.

3. RESULTS AND DISCUSSION

3.1. Coated LPG optical response

The transmission spectrum of the coated LPG presented a wavelength shift pattern of the attenuation bands during the RH test. This shift is due to the swelling/de-swelling properties of the polymeric coating depending the RH conditions [30]. This effect provides noticeable variations in the external refractive index, and therefore it modifies the resonance modes and their attenuation bands. The evolution of this wavelength peak shift of the main attenuation band is shown in Figure 4 a). As the RH values decreased, the peak presented a red shift, ranging from 1513 nm for 80% RH to 1517.7 nm for 20% RH. In a similar way, the peak shifted to 1513 nm again whereas the RH returned to 80% RH.

These pattern was observed for several RH cycles, obtaining a sensitivity ratio of 81.61 pm/%RHunit ($\Delta\lambda_{max}$= -4.7 nm).

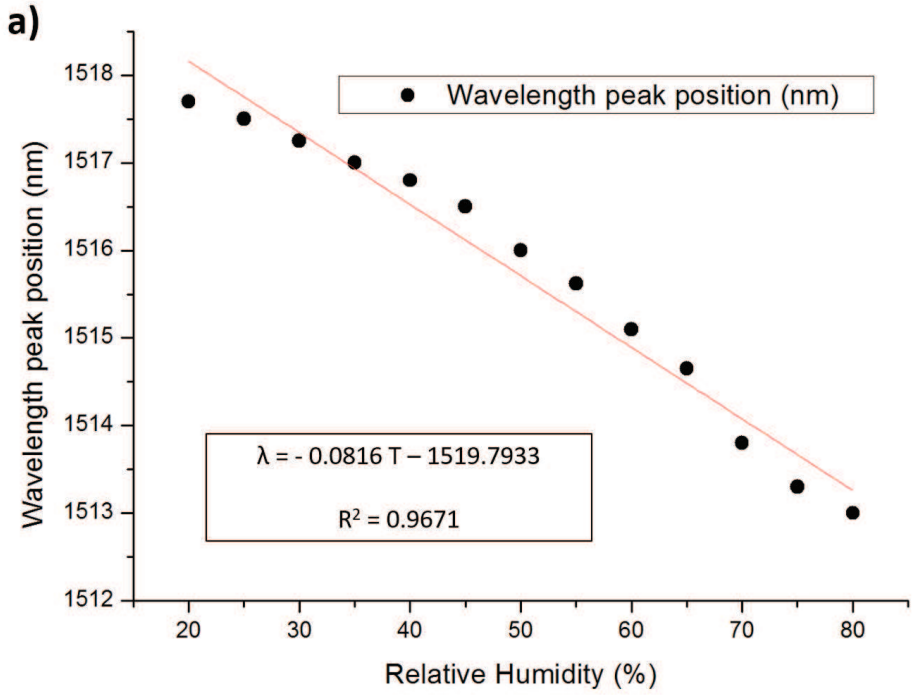

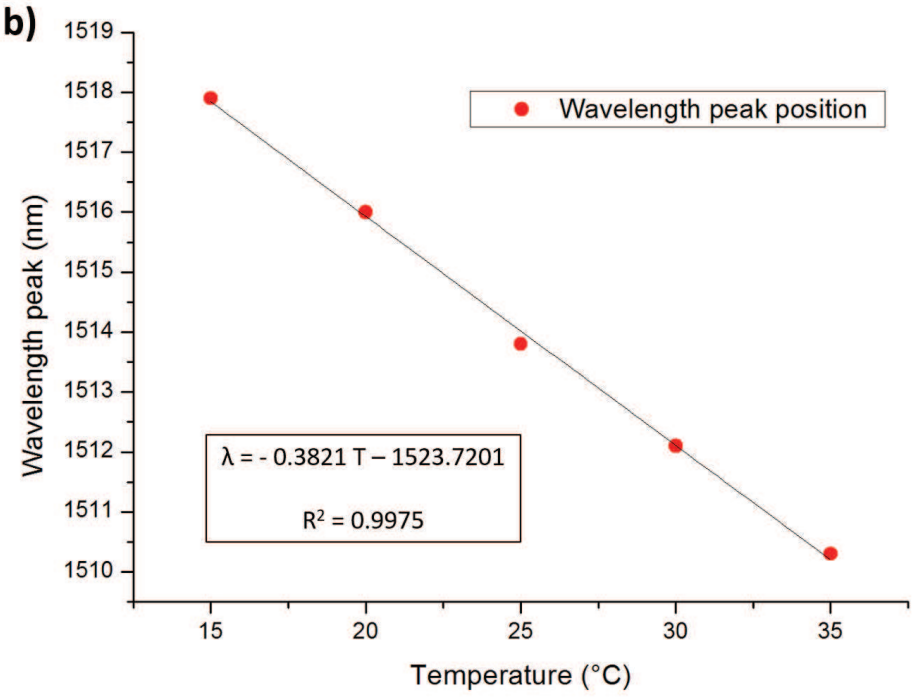

Figure 4. Evolution of the attenuation band wavelength (absolute and shift values) for: a) the RH variation from 20% to 80% and b) temperature variation from 15ºC to 35ºC.

In a further test, the coated LPG was exposed to temperature values ranging from 15ºC to 35ºC at constant RH. This is just a preliminary test used to measure and characterize the LPG intrinsic temperature dependence [7, 31]. Thus, the results showed a linear behavior in the mentioned range, and are represented in Figure 4b). The sensitivity value and the $\Delta\lambda_{max}$ was 398.57 pm/ºC and 7.8 nm, respectively and represent much better values than other recent works with gratings [32-36].

3.2. Partial removal of the coating

Once the RH and temperature tests were finished with the fully coated LPG, the LPG coating was partially removed. A piranha solution (H_2O_2: H_2SO_4 30:70 v/v) was prepared to remove chemically one half of the coating along the grating. This removing process was carefully made step by step so as not to remove more than 50% of the coating according to the theoretical study proposed by Bao et al [29]. The result was a semi-coated LPG as it is shown in Figure 5.

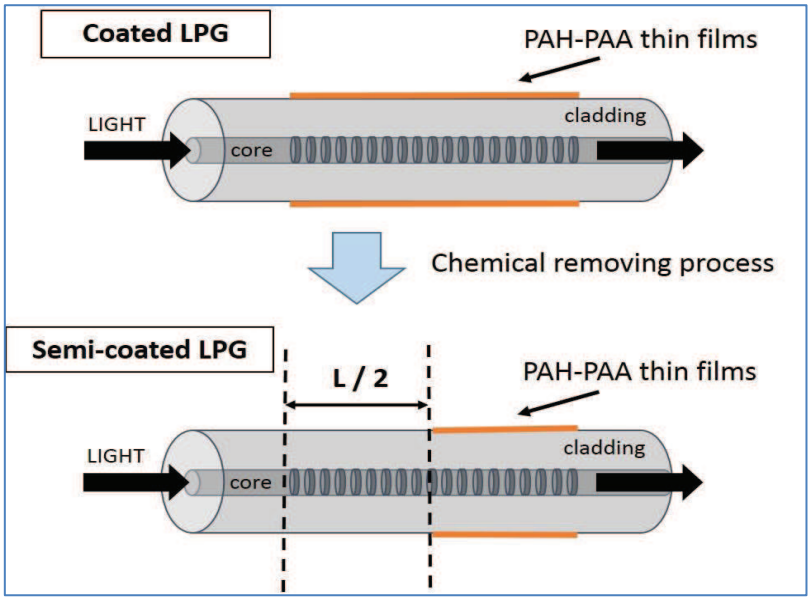

Figure 5. Scheme of the chemical removing process of half of the polymeric coating.

After the chemical treatment, the semi-coated LPG was cleaned and rinsing in several steps with ultrapure water. The transmission spectrum of the new device was taken to observe the modification effect.

The main attenuation band was split into two contributions. On one hand, the coated LPG contribution remained, although its magnitude (optical attenuation in intensity) was reduced significantly owing to the reduction of the coating length along the grating. On the other hand, a second attenuation band appeared because of the removing process. As was expected, this new band corresponds to the half uncoated LPG area, and it was centered in 1547 nm, in the same spectral wavelength of the original uncoated LPG attenuation band. Both contributions have similar weight in magnitude due to their lengths which are approximately half of the total grating length, being this result in agreement with the mentioned theoretical study [29]. This comparison can be observed in Figure 6. It is also shown the Gaussian fitting decomposition of the spectral response of the LPG in two different contributions obtained using a non-linear least square method.

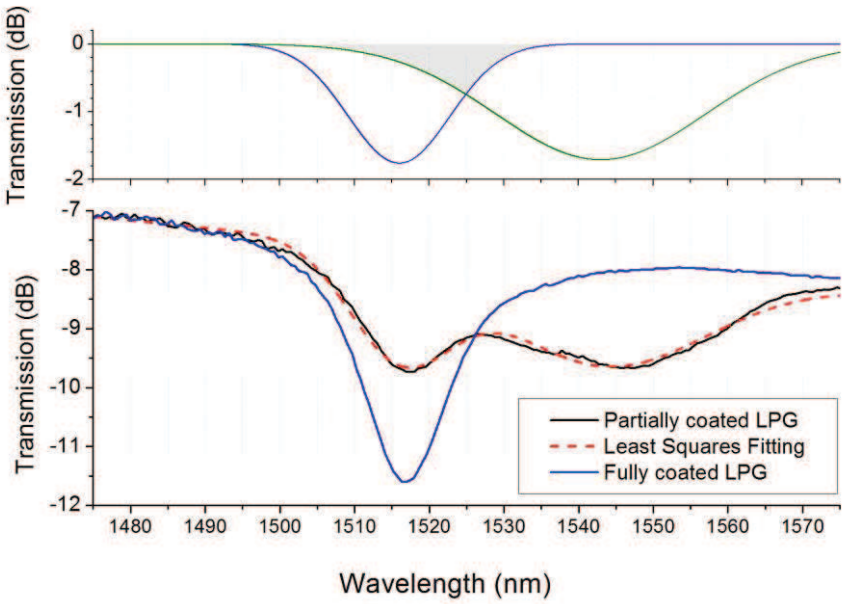

Figure 6. Bottom: Detail of the transmission spectra of the coated LPG and the semi-coated LPG in the range of the main attenuation band (1475-1575 nm). The red dashed line corresponds to the Least-Squares (LS) fitting using a model with two gaussian peaks with baseline subtraction. Top: This graph

shows the individual gaussian contributions of the LS fitting. The overlapping area of both contributions has been highlighted.

Both contribution bands are very close and they present certain mutual overlapping. Figure 6 (bottom), shows the experimental response together with a least square fitting using a model consisting of two gaussian attenuation bands with first order baseline correction. Figure 6 (top) shows the individual attenuation contributions resulting from the least squares fitting, and the overlapping region has been highlighted. This overlapping may have a significant effect in the wavelength-sensitivity of each band. The position of one minimum could be affected by the overlapping tail from the other attenuation band as the minima wavelengths are estimated from the overall transmission spectrum. In other words, a wavelength shift of one band may affect to the experimentally estimated minimum wavelength of the other band.

3.3. Half-coated LPG optical response

The half-coated LPG was submitted to the RH and temperature cycles at the same previous conditions. The optical response showed that both attenuation bands shifted along the RH test. The first attenuation band, attributable to the coated part of the LPG, is centered at 1515 nm and presented the following behavior. The wavelength peak shifted, ranging from 1515.6 nm for 20% RH to 1511.5 for 80% RH (see Figure 7a). From this wavelength shift, the calibration plot was calculated, as it is shown in Figure 7b (black dots). The sensitivity ratio was 63.23 pm/%RH unit with a $\Delta\lambda_{max}$= 4.1 nm for the 20-80% RH range, and registered similar variations in comparison to the fully coated LPG, as expected from the same grating period.

Regarding to the second attenuation band, attributable to the original uncoated LPG, the results showed an opposite behavior respect to the first band. As it was commented previously, the wavelength shift of the first band may affect to the experimentally estimated minimum wavelength of this second band (Figure 6). In this case, as the RH increased, the peak shifted to higher wavelength positions, from

1546.2 nm for 20% RH to 1549.3 nm for 80% RH, as shown in Figure 7a. These evolution peaks are represented in Figure 7b with red dots, and provided a sensitivity ratio of 55.22 pm/%RHunit with $\Delta\lambda_{max}$ = 3.1 nm for the mentioned range.These results were corroborated after multiple RH tests, and showed a high repeatability.

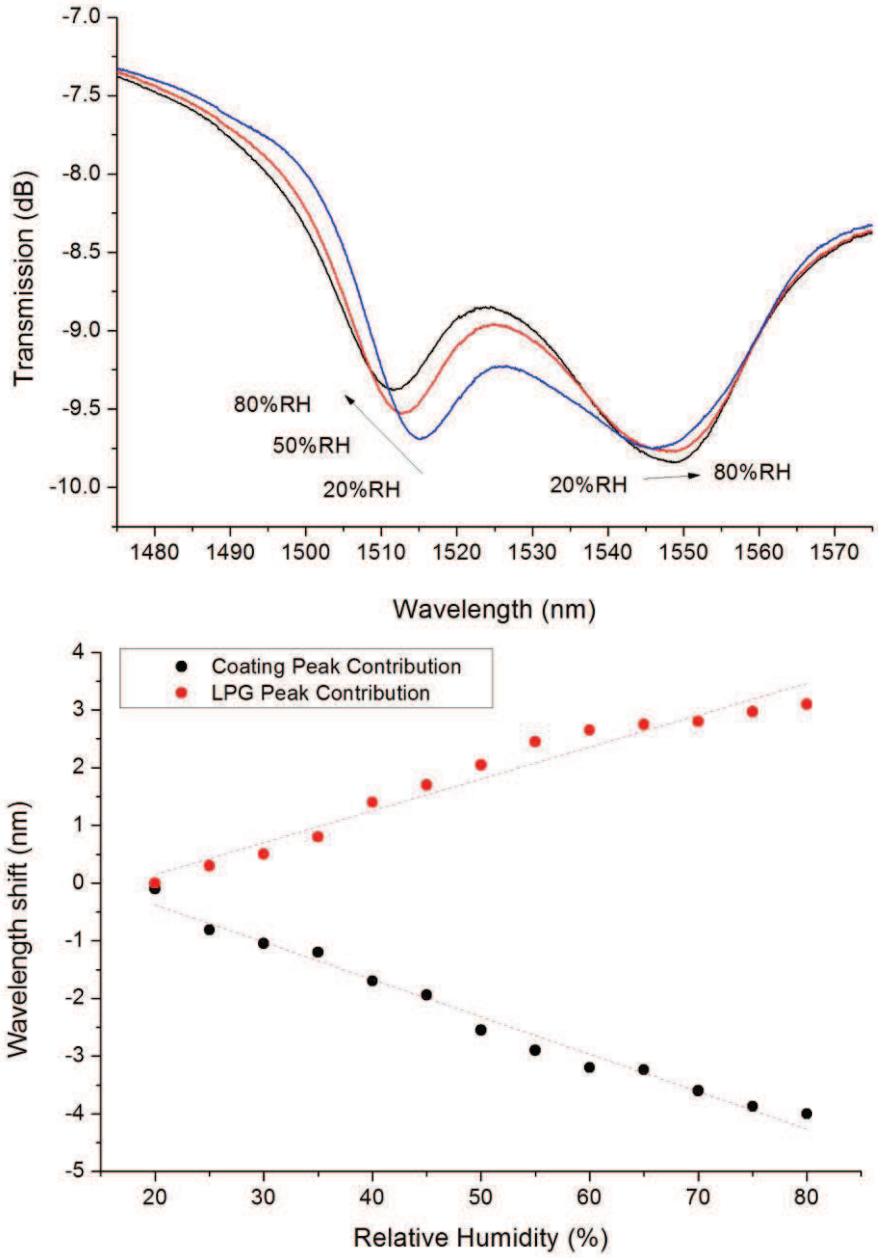

Figure 7. a) Transmission spectra evolution of the partially-coated LPG as the RH is changed. b) Wavelength shift of both attenuation bands during the RH variation: LPG contribution band (red dots), and coating contribution band (black dots).

Afterwards, the half-coated LPG was also monitored under a dynamic range of temperature values, from 25ºC to 85ºC, keeping RH constant values. Both peak contributions presented a linear behavior as the coated LPG case. When temperature increased, then both contribution peaks shifted to lower wavelengths (shown in Figure 8).

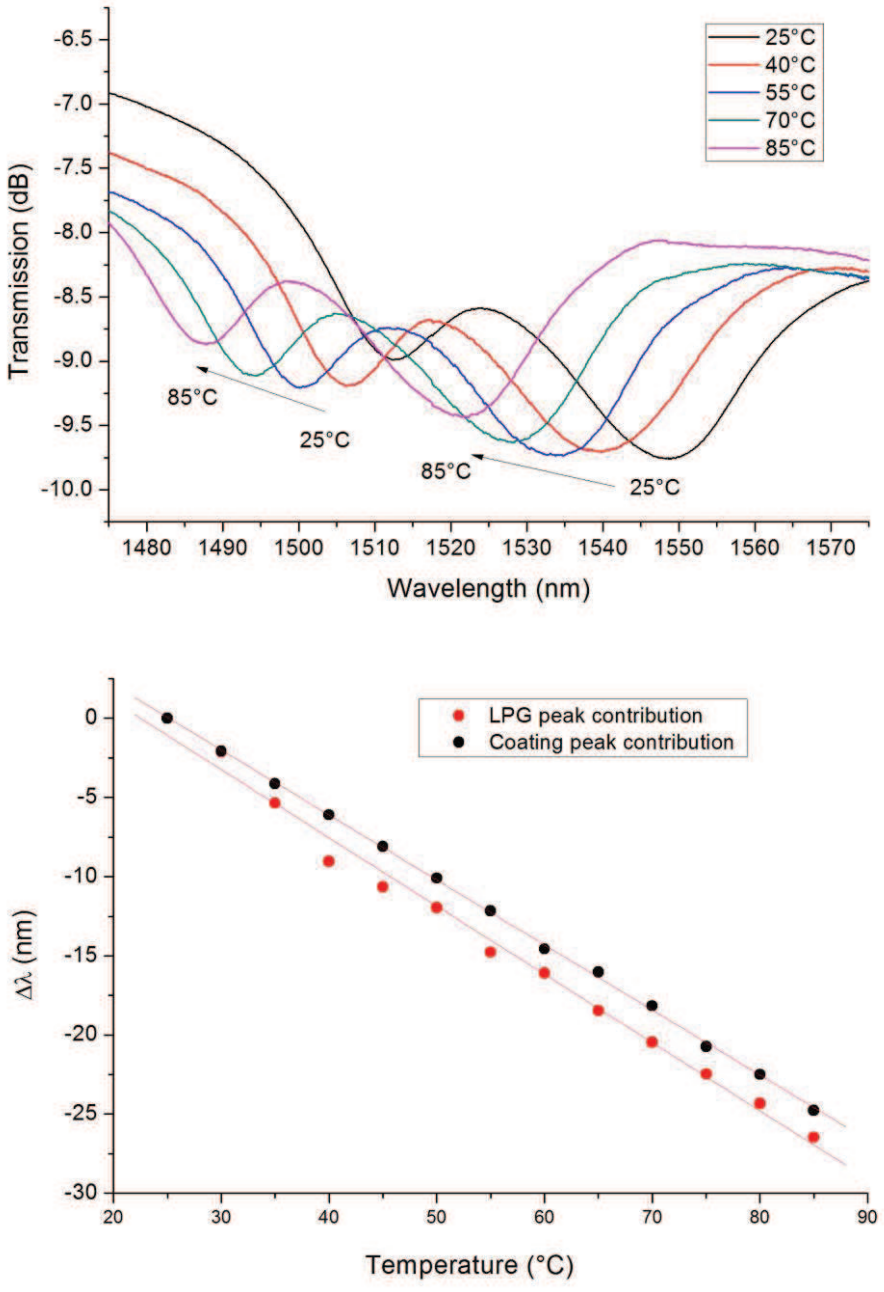

Figure 8. a) Transmission spectra evolution of the partially-coated LPG as the temperature is changed. b) Wavelength shift of both attenuation bands with the temperature variations: LPG contribution band (red dots), and coating contribution band (black dots).

LPG and coating contributions showed very high sensitivity values: 405.09 pm/ºC and 410.66 pm/ºC, respectively. These sensitivities are even better than the coated LPG results, and to the authors´ knowledge, they are the outstanding ratios between recent works reported in literature [32, 36] for a temperature grating based-sensor.

3.4. Simultaneous RH and temperature measurement

Once the RH and temperature tests were performed, and the results were analysed, the resultant behaviour pattern can be characterized as a two equation system for two parameters [25, 37], given by the following matrix expression:

$$\begin{bmatrix} \Delta\lambda_{LPG} \\ \Delta\lambda_{coating} \end{bmatrix} = \begin{bmatrix} k_{TLPG} & k_{RHLPG} \\ k_{Tcoating} & k_{RHcoating} \end{bmatrix} \begin{bmatrix} \Delta T \\ \Delta R_H \end{bmatrix} \quad (1)$$

where k_{TLPG}, k_{RHLPG}, and $k_{Tcoating}$, $k_{RHcoating}$, are the temperature and RH sensitivities of the LPG peak contribution and the coated peak contribution, respectively (see Table 1). The wavelength shift of both peaks are $\Delta\lambda_{LPG}$ and $\Delta\lambda_{coating}$, while the temperature and RH variations are ΔT and ΔR_H, respectively.

Relative Humidity sensitivity (20-80%)		Temperature sensitivity (25-85°C)	
$k_{RHcoating}$	*-63.23 pm / %RH*	$k_{Tcoating}$	*-410.66 pm / ℃*
k_{RHLPG}	*55.22 pm / %RH*	k_{TLPG}	*-405.09 pm / ℃*

Table 1. RH and temperature sensitivity values in the studied ranges.

From (1), and by matrix operations [25, 37], it can be expressed as

$$\begin{bmatrix} \Delta T \\ \Delta R_H \end{bmatrix} = \frac{1}{D} \begin{bmatrix} k_{RHcoating} & -k_{RHLPG} \\ -k_{Tcoating} & k_{TLPG} \end{bmatrix} \begin{bmatrix} \Delta\lambda_{LPG} \\ \Delta\lambda_{coating} \end{bmatrix} \quad (2)$$

where D is the determinant of the matrix which contains temperature and RH sensitivities ($D= k_{TLPG}\cdot k_{RHcoating} - k_{RHLPG}\cdot k_{Tcoating}$). Therefore, the specific expression for the half-coated LPG sensor, using the coefficients of the table 1, is given by

$$\begin{bmatrix} \Delta T \\ \Delta R_H \end{bmatrix} = 20.70801 \begin{bmatrix} -0.06323 & -0.05522 \\ 0.41066 & -0.40509 \end{bmatrix} \begin{bmatrix} \Delta\lambda_{LPG} \\ \Delta\lambda_{coating} \end{bmatrix} \quad (3)$$

The system mechanism proposed in (3) was checked varying the RH and temperature conditions. The sensitive system was tested in an experiment in which a partially coated LPG is submitted firstly to a 20-80% RH variation at a constant temperature of 25ºC. Afterwards the same sensor was monitored under a 25-80ºC at a constant RH of 40%. The experimental results of the position of both optical transmission minima were recorded and processed using Eq. 3, and the results are shown in Figure 9.

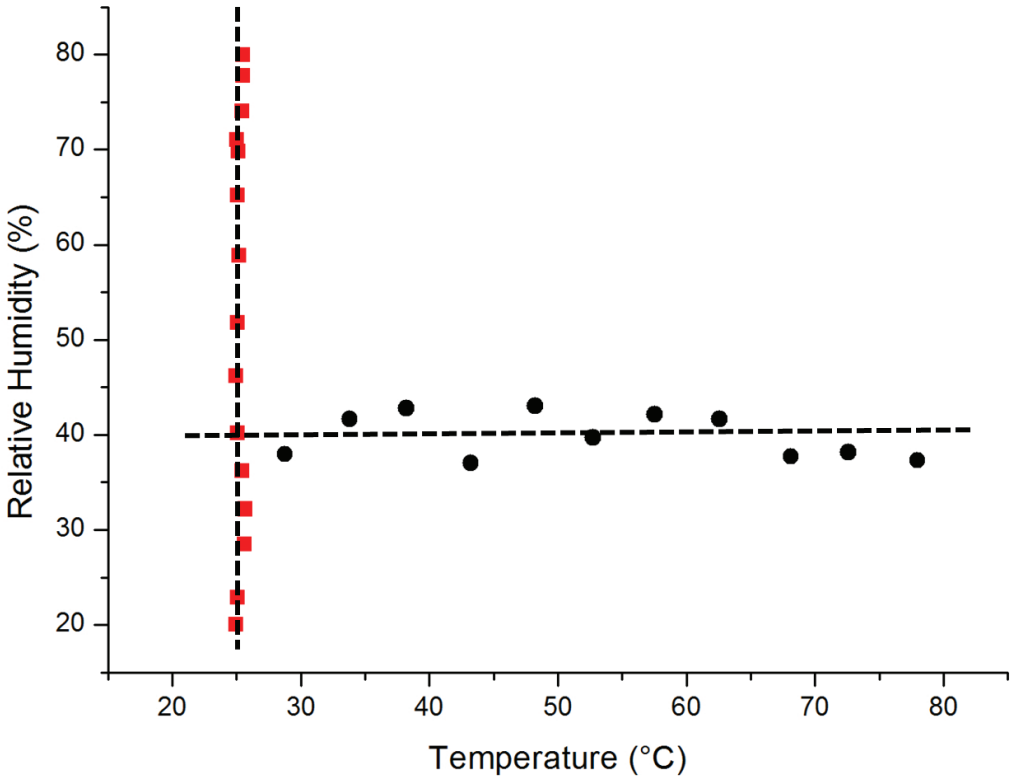

Figure 9. Half-coated LPG sensor response from equation (3) for RH variation at constant temperature level, and for temperature variation at constant RH level. Dash lines represent the trend of experimental data in both cases.

As it is shown in Figure 9, the experimental results show an excellent fit in temperature for any RH variations in the 20%-80% range. The standard deviation obtained in this case is 0.244ºC. On the other hand, the RH values recorded for different temperatures showed a higher standard deviation of 2.352%RH. These variabilities are directly related by the performance of the climatic chamber and the

intrinsic instability of the RH as temperature was changed. Nevertheless, the wavelength-based measurement system proposed in this work have succeeded in the extraction of the temperature and RH measurements from the absolute wavelengths of the two adjacent minima obtained from a single partially coated LPG sensor.

4. CONCLUSIONS

A temperature and humidity sensor based on a half-coated LPG is presented. Firstly, the variation of the optical response of a LPG was studied when a polymeric LbL overlay was built-up onto the cladding. In a further step, half of the LbL coating was chemically removed, resulting a half-coated LPG. The new half-coated LPG provided a split of the attenuation band observed in the fully coated LPG into two components: one attributable to the fully coated LPG, centered in 1515 nm, and other, attributable to the uncoated LPG, centered in 1547 nm. This device was also exposed to humidity and temperature cycles, and the spectra were studied.

Both attenuation bands presented wavelength shift as the RH changes. The peak centered in 1515 nm had a similar behavior than the coated LPG. In contrast, the other peak presented an opposite shift variation. The LPG-based sensor was also characterized under different temperature conditions. All results were analyzed, obtaining a dual-wavelength sensing mechanism based on the shifts of both peaks. The dual-wavelength based measurement provided a simultaneous monitoring of RH and temperature, with sensitivity ratios of 63.23 pm/%RH and 410.66 pm/ºC for the attenuation band corresponding to the coated contribution, and 55.22 pm/%RH and 405.09 pm/ºC for the attenuation band corresponding to the uncoated grating.

This novel, simple and cost-efficient approach could be applied in many coated LPG based sensors already developed to measure more than one magnitude, and also it could be a good alternative to the cascaded-LPGs sensing systems where the use of at least two LPGs is required to monitor simultaneously two different parameters.

ACKNOWLEDGEMENTS

This work was supported in part by the Spanish Ministry of Economy and Competitiveness –through the projects CICYT-FEDER TEC2013-43679-R and TEC2014-60378-C2-1-R. It was also supported by a UPNA pre-doctoral research grant, by the Program of International Excellence Campus VLC/Campus, by the grant of program SANTIAGO GRISOLÍA, and by the Research Excellency Award Program GVA PROMETEO 2013/012.

FIGURE CAPTIONS

Figure 1. Scheme of a LPG, indicating their parameters, and its characteristic spectrum when the light goes through the grating.

Figure 2. Experimental setup to monitor the optical sensor response.

Figure 3. Evolution of the LPG spectrum for the main attenuation band during the LbL assembly process.

Figure 4. Evolution of the attenuation band wavelength (absolute and shift values) for: a) RH variation from 20% to 80% and b) temperature variation from 15ºC to 35ºC.

Figure 5. Scheme of the chemical removing process of half of the polymeric coating.

Figure 6. Detail of the transmission spectra of the coated LPG and the semi-coated LPG in the range of the main attenuation band (1475-1575 nm).

Figure 7. a) Transmission spectra evolution of the partially-coated LPG as the RH is changed. b) Wavelength shift of both attenuation bands during the RH variation: uncoated LPG contribution band (red dots), and coated LPG contribution band (black dots).

Figure 8. a) Transmission spectra evolution of the partially-coated LPG as the temperature is changed. b) Wavelength shift of both attenuation bands with the temperature variations: LPG contribution band (red dots), and coating contribution band (black dots).

Figure 9. Half-coated LPG sensor response from equation (3) for RH variation at constant temperature level, and for temperature variation at constant RH level. Dash lines represent the trend of experimental data in both cases.

TABLE CAPTIONS

Table 1. RH and temperature sensitivity values in the studied ranges.

REFERENCES

[1] R. Jindal, S. Tao, J.P. Singh, P.S. Gaikwad, High dynamic range fiber optic relative humidity sensor, Optical Engineering. 41 (2002) 1093-1096.

[2] B. Culshaw, Optical Fiber Sensor Technologies: Opportunities and - Perhaps - Pitfalls, J. Lightwave Technol. 22 (2004) 39-50.

[3] T.G. Giallorenzi, J.A. Bucaro, A. Dandridge, G.H. Siegel Jr., J.H. Cole, S.C. Rashleigh, R.G. Priest, Optical Fiber Sensor Technology. IEEE J. Quant. Electron. QE-18 (1982) 626-665.

[4] I. Del Villar, A.B. Socorro, M. Hernaez, J.M. Corres, C.R. Zamarreño, P. Sanchez, F.J. Arregui, I.R. Matias, Sensors Based on Thin-Film Coated Cladding Removed Multimode Optical Fiber and Single-Mode Multimode Single-Mode Fiber: A Comparative Study, Journal of Sensors, 2015,(2015), 763762.

[5] V. Bhatia, A.M. Vengsarkar, Optical fiber long-period grating sensors, Opt. Lett. 21 (1996) 692-694.

[6] A.D. Kersey, M.A. Davis, H.J. Patrick, M. LeBlanc, K.P. Koo, C.G. Askins, M.A. Putnam, E.J. Friebele, Fiber grating sensors, J. Lightwave Technol. 15 (1997) 1442-1462.

[7] S.W. James, R.P. Tatam, Optical fibre long-period grating sensors: Characteristics and application, Measurement Science and Technology. 14 (2003) R49-R61.

[8] A.M. Vengsarkar, P.J. Lemaire, J.B. Judkins, V. Bhatia, T. Erdogan, J.E. Sipe, Long-period fiber gratings as band-rejection filters, J. Lightwave Technol. 14 (1996) 58-64.

[9] I. Del Villar, J.M. Corres, M. Achaerandio, F.J. Arregui, I.R. Matias, Spectral evolution with incremental nanocoating of long period fiber gratings, Optics Express. 14 (2006) 11972-11981.

[10] X. Zhang, H. Chen, H. Zhang, Layer-by-layer assembly: From conventional to unconventional methods, Chemical Communications. (2007) 1395-1405.

[11] Z. Zhao, Y. Duan, A low cost fiber-optic humidity sensor based on silica sol-gel film, Sensors and Actuators, B: Chemical. 160 (2011) 1340-1345.

[12] P. Sigmund, Elements of sputtering theory, Nanofabrication by Ion-Beam Sputtering: Fundamentals and Applications. (2012) 1-40.

[13] A. Urrutia, J. Goicoechea, P.J. Rivero, I.R. Matías, F.J. Arregui, Electrospun nanofiber mats for evanescent optical fiber sensors, Sensors and Actuators, B: Chemical. 176 (2013) 569-576.

[14] D. Viegas, J. Goicoechea, J.M. Corres, J.L. Santos, L.A. Ferreira, F.M. Arajo, I.R. Matias, A fibre optic humidity sensor based on a long-period fibre grating coated with a thin film of SiO2 nanospheres, Measurement Science and Technology. 20 (2009).

[15] J.M. Corres, I. Del Villar, I.R. Matias, F.J. Arregui, Two-layer nanocoatings in long-period fiber gratings for improved sensitivity of humidity sensors, IEEE Transactions on Nanotechnology. 7 (2008) 394-400.

[16] C. Berrettoni, C. Trono, V. Vignoli, F. Baldini, Fibre tip sensor with embedded FBG-LPG for temperature and refractive index determination by means of the simple measurement of the FBG characteristics, Journal of Sensors. 2015 (2015), 491391.

[17] J.M. Corres, I. Del Villar, I.R. Matias, F.J. Arregui, Fiber-optic pH-sensors in long-period fiber gratings using electrostatic self-assembly, Opt. Lett. 32 (2007) 29-31.

[18] A. Trouillet, E. Marin, C. Veillas, Fibre gratings for hydrogen sensing, Measurement Science and Technology. 17 (2006) 1124-1128.

[19] X. Wei, T. Wei, H. Xiao, Y.S. Lin, Nano-structured Pd-long period fiber gratings integrated optical sensor for hydrogen detection, Sensors and Actuators, B: Chemical. 134 (2008) 687-693.

[20] M. Konstantaki, A. Klini, D. Anglos, S. Pissadakis, An ethanol vapor detection probe based on a ZnO nanorod coated optical fiber long period grating, Optics Express. 20 (2012) 8472-8484.

[21] S. Korposh, R. Selyanchyn, W. Yasukochi, S.-. Lee, S.W. James, R.P. Tatam, Optical fibre long period grating with a nanoporous coating formed from silica nanoparticles for ammonia sensing in water, Mater. Chem. Phys. 133 (2012) 784-792.

[22] S.M. Topliss, S.W. James, F. Davis, S.P.J. Higson, R.P. Tatam, Optical fibre long period grating based selective vapour sensing of volatile organic compounds, Sensors and Actuators, B: Chemical. 143 (2010) 629-634.

[23] L. Marques, F.U. Hernandez, S. Korposh, M. Clark, S. Morgan, S. James, R.P. Tatam, Sensitive protein detection using an optical fibre long period grating sensor anchored with silica core gold shell nanoparticles, Proceedings of SPIE - The International Society for Optical Engineering. 9157 (2014).

[24] A. Urrutia, J. Goicoechea, F.J. Arregui, Optical fiber sensors based on nanoparticle-embedded coatings, Journal of Sensors, 2015 (2015), 805053.

[25] D. Viegas, M. Hernaez, J. Goicoechea, J.L. Santos, F.M. Araújo, F. Arregui, I.R. Matias, Simultaneous measurement of humidity and temperature based on an SiO 2-nanospheres film deposited on a long-period grating in-line with a fiber Bragg grating, IEEE Sensors Journal. 11 (2011) 162-166.

[26] S.W. James, S. Korposh, S.-. Lee, R.P. Tatam, A long period grating-based chemical sensor insensitive to the influence of interfering parameters, Optics Express. 22 (2014) 8012-8023.

[27] F.J. Arregui, I.R. Matías, K.L. Cooper, R.O. Claus, Simultaneous measurement of humidity and temperature by combining a reflective intensity-based optical fiber sensor and a fiber bragg grating, IEEE Sensors Journal. 2 (2002) 482-487.

[28] I. Del Villar, F.J. Arregui, I.R. Matias, A. Cusano, D. Paladino, A. Cutolo, Fringe generation with non-uniformly coated long-period fiber gratings, Optics Express. 15 (2007) 9326-9340.

[29] J. Bao, P. Cheng, H. Zhao, J. Wang, L. Wu, Spectral characteristics of a two-section multilayer long-period fiber grating sensor, Optik. 125 (2014) 4689-4693.

[30] K.E. Secrist, A.J. Nolte, Humidity swelling/deswelling hysteresis in a polyelectrolyte multilayer film, Macromolecules. 44 (2011) 2859-2865.

[31] X. Shu, L. Zhang, I. Bennion, Sensitivity characteristics of long-period fiber gratings, J. Lightwave Technol. 20 (2002) 255-266.

[32] M.A. Gonzalez-Reyna, E. Alvarado-Mendez, J.M. Estudillo-Ayala, E. Vargas-Rodriguez, M.E. Sosa-Morales, J.M. Sierra-Hernandez, D. Jauregui-Vazquez, R. Rojas-Laguna, Laser temperature sensor based on a fiber bragg grating, IEEE Photonics Technology Letters. 27 (2015) 1141-1144.

[33] V.R. Mamidi, S. Kamineni, L.N.S.P. Ravinuthala, V. Thumu, V.R. Pachava, Characterization of encapsulating materials for fiber bragg grating-based temperature sensors, Fiber and Integrated Optics. 33 (2014) 325-335.

[34] D. Zhang, J. Wang, Y. Wang, X. Dai, A fast response temperature sensor based on fiber Bragg grating, Measurement Science and Technology. 25 (2014).

[35] W. Zhang, Z. Ying, S. Yuan, Z. Tong, A fiber laser sensor for liquid level and temperature based on two taper structures and fiber Bragg grating, Opt. Commun. 342 (2015) 243-246.

[36] Q. Zhou, T. Ning, X. Wen, C. Li, A fiber Bragg grating sensor for temperature-stress simultaneous measurement, Hongwai yu Jiguang Gongcheng/Infrared and Laser Engineering. 44 (2015) 1024-1027.

[37] O. Frazao, L. A. Ferreira, F. M. Araujo, J. L. Santos, Applications of fiber optic grating technology to multi-parameter measurement, Fiber and Integrated Optics, 24, (2005) 227-244.